A general design algorithm for low optical loss adiabatic connections in waveguides

Tong Chen, Hansuek Lee, Jiang Li, and Kerry J. Vahala*

T. J. Watson Laboratory of Applied Physics, California Institute of Technology, Pasadena, California, 91125, USA

*vahala@caltech.edu

Abstract: Single-mode waveguide designs frequently support higher order transverse modes, usually as a consequence of process limitations such as lithography. In these systems, it is important to minimize coupling to higher-order modes so that the system nonetheless behaves single mode. We propose a variational approach to design adiabatic waveguide connections with minimal intermodal coupling. An application of this algorithm in designing the "S-bend" of a whispering-gallery spiral waveguide is demonstrated with approximately 0.05 dB insertion loss. Compared to other approaches, our algorithm requires less fabrication resolution and is able to minimize the transition loss over a broadband spectrum. The method can be applied to a wide range of turns and connections and has the advantage of handling connections with arbitrary boundary conditions.

OCIS codes: (230.7370) Waveguide; (230.7390) Waveguide, planar; (220.0220) Optical design and fabrication.

References and links

1. F. Ladouceur and P. Labeye, "A new gerenal approach to optical waveguide path design," J. Lightwave Tech. **13**, 481–491 (1995).
2. R. Adar, M. Serbin, and V. Mizrahi, "Less than 1 dB per meter propagation loss of silica waveguides measured using a ring resonator," J. Lightwave Tech. **12**, 1369–1372 (1994).
3. K. Takada, H. Yamada, Y. Hida, Y. Ohmori, and S. Mitachi, "Rayleigh backscattering measurement of 10 m long silica-based waveguides," Electron. Lett. **32**, 1665–1667 (1996).
4. J. F. Bauters, M. Heck, D. John, D. Dai, M. Tien, J. S. Barton, A. Leinse, R. G. Heideman, D. J. Blumenthal, and J. E. Bowers, "Ultra-low-loss high-aspect-ratio Si_3N_4 waveguides," Opt. Express **19**, 3163–3174 (2011).
5. H. Lee, T. Chen, J. Li, O. Painter, and K. Vahala, "Ultra-low-loss optical delay line on a silicon chip," Nat. Commun. **3**, doi:10.1038/ncomms1876 (2012).
6. J. F. Bauters, M. Heck, D. D. John, J. S. Barton, C. M. Bruinink, A. Leinse, R. Heideman, D. J. Blumenthal, and J. E. Bowers, "Planar waveguides with less than 0.1 dB/m propagation loss fabricated with wafer bonding," Opt. Express **19**, 24090–24101 (2011).
7. E. Marcatilli, "Bends in optical dielectric guides," Bell Syst. Tech. J. **48**, 2103–2132 (1969).
8. R. Baets and P. Lagasse, "Loss calculation and design of arbitrarily curved integrated-optic waveguides," J. Opt. Soc. Am. **73**, 177–182 (1983).
9. V. Subramaniam, G. De Brabander, D. Naghski, and J. Boyd, "Measurement of mode field profiles and bending and transition losses in curved optical channel waveguides," J. Lightwave Tech. **15**, 990–997 (1997).
10. W. Gambling, H. Matsumura, and C. Ragdale, "Field deformation in a curved single-mode fiber," Electron. Lett. **14**, 130–132 (1978).
11. T. Kitoh, N. Takato, M. Yasu, and M. Kawachi, "Bending loss reduction in silica-based waveugide by using lateral offests," J. Lightwave Tech. **13**, 555–562 (1995).
12. A. Melloni, P. Monguzzi, R. Costa, and M. Martinelli, "Design of curved waveugide: the matched bend," J. Opt. Soc. Am. A **20**, 130–137 (2003).

#171778 - $15.00 USD Received 3 Jul 2012; revised 6 Sep 2012; accepted 7 Sep 2012; published 20 Sep 2012

13. T. Kominato, Y. Hida, M. Itoh, H. Takahashi, S. Sohma, T. Kitoh, and Y. Hibino, "Extremely low-loss (0.3 dB/m) and long silica-based waveguides with large width and clothoid curve connection," in Proceedings of ECOC TuI.4.3 (2004).
14. D. Meek and J. Harris, "Clothoid spline transition spirals," Math. Comp. **59**, 117–133 (1992).
15. D. J. Walton, "Spiral spline curves for highway design," Microcomputers in Civil Engineering **4**, 99–106 (1989).
16. K. G. Bass, "The use of clothoid templates in highway design," Transportation Forum **1**, 47–52 (1984).
17. S. Fleury, P. Soueres, J. P. Laumond, and R. Chatila, "Primitives for smoothing mobile robot trajectories," IEEE Trans. Robot. Autom. **11**, 441–448 (1995).
18. J. McCrae and K. Singh, "Sketching piecewise clothoid curves," Computers & Graphics **33**, 452–461 (2008).
19. K. Takada, H. Yamada, Y. Hida, Y. Ohmori, and S. Mitachi, "New waveguide fabrication techniques for next-generation plcs," NTT Technical Review **3**, 37–41 (2005).
20. A. W. Snyder, "Radiation losses due to variations of radius on dielectric or optical fibers," IEEE Trans. Microwave Theory Tech. **18**, 608–615 (1970).
21. A. W. Snyder, "Excitation and scattering of modes on a dielectic or optical fiber," IEEE Trans. Microwave Theory Tech. **17**, 1138–1144 (1969).
22. M. Heiblum and J. Harris, "Analysis of curved optical waveguides by conformal transformation," IEEE J. Quantum Electron. **11**, 75–83 (1975).
23. R. Ulrich, "Fiber-optic rotation sensing with low drift," Opt. Express **5**, 173–175 (1980).
24. C. Ciminelli, F. Dell'Olio, C. Campanella, and M. Armenise, "Photonic technologies for angular velocity sensing," Adv. Opt. Photon. **2**, 370–404 (2010).
25. W. Chang, ed., *RF Photonic Technology in Optical Fiber Links* (Cambridge University Press, 2002).
26. X. Yao and L. Maleki, "Optoelectronic microwave oscillator," J. Opt. Soc. Am. B **13**, 1725–1735 (1996).
27. C. Koos, P. Vorreau, T. Vallaitis, P. Dumon, W. Bogaerts, R. Baets, B. Esembeson, I. Biaggio, T. Michinobu, F. Diederich, W. Freude, and J. Leuthold, "All-optical high-speed signal processing with silicon-organic hybrid slot waveguides," Nat. Photonics **3**, 216–219 (2009).
28. R. L. Levien, "From spiral to spline: Optimal techniques in interactive curve design," Ph.D. thesis, UC Berkeley (2009).
29. S. Ohlin, *Splines for Engineers* (Eurographics Association, 1987).
30. B. Soller, D. Gifford, M. Wolfe, and M. Froggatt, "High resolution optical frequency domain reflectometry for characterization of components and assemblies," Opt. Express **13**, 666–674 (2005).
31. H. Lee, T. Chen, J. Li, O. Painter, and K. Vahala, "Chemically etched ultrahigh-Q wedge-resonator on a silicon chip," Nat. Photonics **6**, 369–373 (2012).
32. M. Cai, O. Painter, and K. J. Vahala, "Observation of critical coupling in a fiber taper to silica-microsphere whispering gallery mode system," Phys. Rev. Lett. **85**, 1430–1432 (2000).
33. H. Rokhsari and K. J. Vahala, "Ultralow loss, high q, four port resonant couplers for quantum optics and photonics," Phys. Rev. Lett. **92**, 253905 (2004).

1. Introduction

Progress in optical communications has motivated much research in optical circuits composed of basic elements such as modulators, switches and splitters. In designing any type of integrated optical circuit, linking two given points or elements with minimal loss is a universal problem [1]. It is becoming even more important in the light of the recent development of ultra-low-loss optical waveguides [2–6]. With propagation loss less than $0.1\,\mathrm{dB/m}$ [5, 6], the additional loss imposed by connections in these structures must be addressed carefully. The current design strategy is normally based on piece-wise construction from a certain family of curves, such as ellipses and sinusoidal curves [1,7,8]. However, it is not clear that these families will always provide the best possible solution to the general problem of linking two points in an arbitrary optical circuit. Herein, we propose a novel algorithm to the optical connection design. The design algorithm minimizes the transition loss by avoiding excitation of higher-order optical modes. It is physically based and applicable to any waveguide connection (single mode or multimode) between two points in a photonics circuit. The approach is flexible enough to handle arbitrary boundary conditions.

An ideal design algorithm will minimize two types of loss: bending loss and transition loss. The first mechanism is a result of radiative loss present in any bent waveguide. The second mechanism, which is more critical in connection design, comes from the abrupt change or discontinuity of curvature in the connection. It includes not only mismatch of overlap in the

#171778 - $15.00 USD Received 3 Jul 2012; revised 6 Sep 2012; accepted 7 Sep 2012; published 20 Sep 2012

propagating mode at the joint points but also the intermode power exchange (cross talk) caused by the variation of curvature along the connection waveguide path. This cross talk can cause distortion via multimode interference. Because bending loss is most readily reduced by making the bend radius larger or by increasing the mode confinement, it is the connection loss that is the primary focus here. However, the proposed algorithm, by minimizing all intermode coupling, actually minimizes both bending loss and transition loss [9, 10].

A generalized waveguide connection is illustrated in Fig. 1 with different curvatures at the terminals of waveguides A and B. In prior work, several different methods have been applied to reduce the insertion loss of this connection. In the offset approach, a small lateral offset in waveguides of different curvature (but having the same tangent) is applied to improve mode overlap [11]. However, this method always results in some mismatch of the modes and also requires high resolution fabrication. In the matched bent approach, the connection is designed to minimize the leaky-mode excitation at the end of the bend [12]. In particular, if the length of the bent waveguide is a multiple of the beat length of the fundamental and a higher-order mode, then only the fundamental mode is present at the output of the bend. This approach has the side effect of introducing a wavelength dependence into the design. In another method, the curvature is smoothly transformed between the endpoints using specialized curves [13]. One such curve is a clothoid curve [14], which is widely used in highway design [15, 16], robot path planning [17] and computer graphics [18]. However, this method is not general enough to minimize loss in problems containing other constraints such as footprint minimization and general boundary conditions. Our algorithm, in contrast, is based on loss minimization and connection designs satisfying arbitrary boundary conditions. A variational approach is introduced to achieve the optimal curve connecting two waveguide endpoints having specified curvature and tangent vectors. Section 2 introduces our general design algorithm and section 3 describes the experimental result to validate our algorithm.

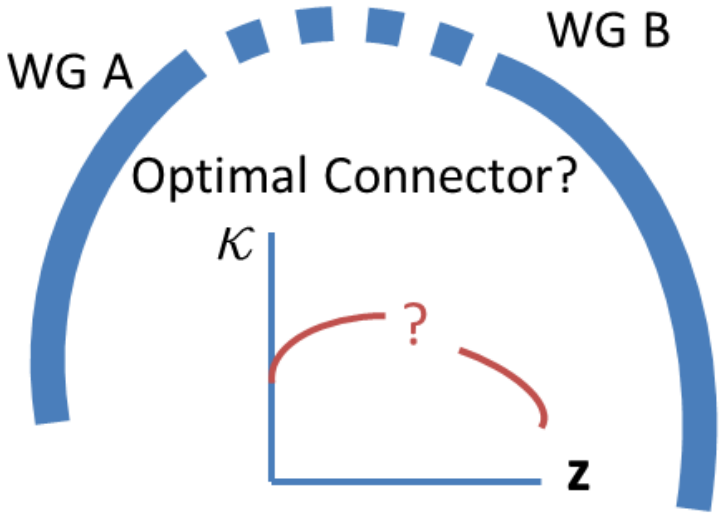

Fig. 1: An illustration of the generic connection design problem. Waveguides A and B are shown linked by the connection waveguide (dashed). To create a low insertion loss, coupling to higher-order modes must be reduced at the connecting points as well as through out the transition. The inset shows the curvature (κ) versus path length, z.

#171778 - $15.00 USD Received 3 Jul 2012; revised 6 Sep 2012; accepted 7 Sep 2012; published 20 Sep 2012

2. Design Algorithm

2.1. Overview

In a straight waveguide, the fundamental mode is centered in the waveguide, while it is slightly shifted from center in a curved waveguide [19]. This mismatch results in loss when the light transitions between two segments with discontinuous curvature. To this end, we require the junction of the connection region to the waveguides A and B to feature a continuous curvature. Likewise, the curvature is required to be continuous along the connection waveguide. Even with the continuous curvature, the evolution of curvature itself along the connection waveguide can introduce inter-mode power transfer [20, 21]. Accordingly, the slow or adiabatic evolution of curvature along the connector is desirable.

Conformal mapping provides a way to both simplify the discussion and provide a more intuitive understanding of the light-wave evolution [22]. If $n(x,y)$ denotes the transverse refractive index of the waveguide, $\kappa(z)$ is the curvature, (x,y) are the transverse coordinates ($x = R_1$ and $x = R_2$ at the inner and outer boundary) and z is the coordinate along the direction of propagation, then using the conformal transformation (see Fig. 2),

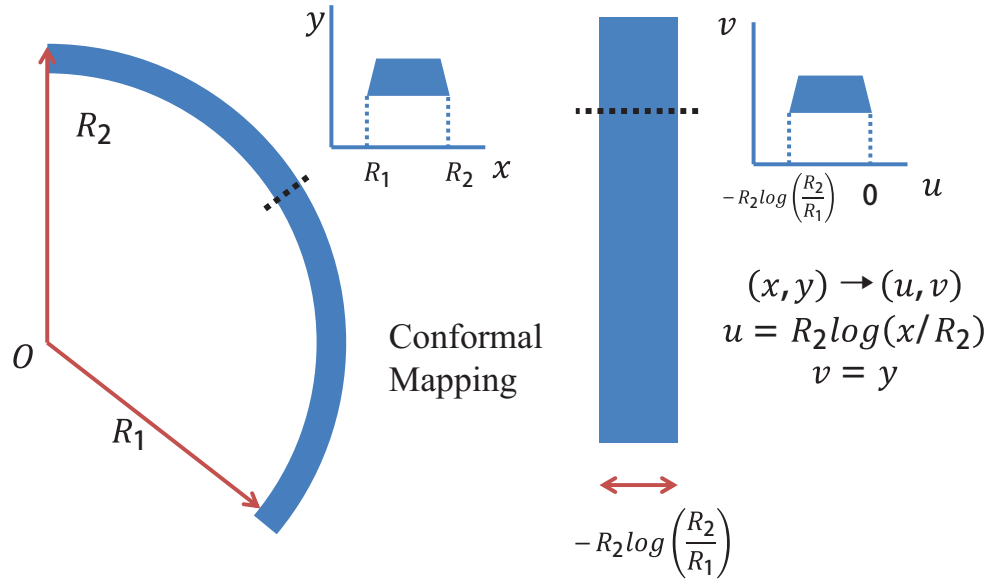

Fig. 2: Conformal mapping between a bent waveguide and a straight waveguide. The transverse refractive index, $n(x,y)$, of the curved waveguide is mapped to $n^2_{eq}(u,v,z) = n^2(u,v)e^{2u\kappa(z)}$ for a straight guide.

$$(x,y) \rightarrow (u,v): \; u = R_2 \log(x/R_2), \; v = y \tag{1}$$

one can show that a bent waveguide with curvature $\kappa(z)$ behaves like a straight waveguide with a refractive index profile [22] given by,

$$n^2_{eq}(u,v,z) = n^2(u,v)e^{2u\kappa(z)} \tag{2}$$

With this mapping, the original problem can be transformed to the equivalent problem of designing the refractive index profile in a non-uniform straight waveguide.

The transition loss can be calculated from coupled-mode theory. We consider a medium with

#171778 - $15.00 USD Received 3 Jul 2012; revised 6 Sep 2012; accepted 7 Sep 2012; published 20 Sep 2012

general dielectric constant $\varepsilon(\vec{r})$ and constant permeability μ. The fields are expressed by the superposition of local normal modes, $\{\vec{e}_p(x,y), \vec{h}_p(x,y)\}$, having propagation constants $\{\beta_p\}$

$$\vec{E} = \sum_p A(\beta_p,z)\vec{e}_p(x,y) \tag{3}$$

$$\vec{H} = \sum_p A(\beta_p,z)\vec{h}_p(x,y) \tag{4}$$

with orthonormal condition

$$\iint_S \hat{z}\cdot(\vec{e}_p \times \vec{h}_q^*)\, dS = \delta_{pq} \tag{5}$$

where $\hat{z}$ is the unit vector along the axis of propagation and "S" represents the local surface area that is normal to the axis of propagation. For slow variation in ε, the coupling coefficient $C(\beta_p,\beta_q)$ between two modes p and q is given by ($q \neq p$)

$$\begin{aligned} C(\beta_p,\beta_q) &= \frac{1}{4}\iint_S \hat{z}\cdot\big(\vec{e}_q \times \frac{\partial \vec{h}_p^*}{\partial z} - \vec{e}_p^* \times \frac{\partial \vec{h}_q}{\partial z}\big)\, dS \\ &= \frac{\omega}{4(\beta_p-\beta_q)}\iint_S \big(\vec{e}_q\cdot\vec{e}_p^*\big)\frac{\partial \varepsilon}{\partial z}\, dS \end{aligned} \tag{6}$$

where ω is the optical frequency in radians/sec. We see that the coupling is directly proportional to $\frac{\partial \varepsilon}{\partial z}$ and only exists between the modes with the same polarizations. Now consider a region from z_0 to z_1 and suppose that at $z = z_0$ the only non-zero modal amplitude is $A(\beta_p,z_0)$. To leading order, the propagation solution is given by:

$$A(\beta_q,z_1) \sim A(\beta_p,z_0)\int_{z_0}^{z_1} C(\beta_p,\beta_q)\exp\big(i(\beta_p-\beta_q)z\big)dz \times \exp\big(-i\int_{z_0}^{z_1}\beta_q(z)dz\big) \tag{7}$$

Thus, power transfer from mode p to q is found to be proportional to $(\frac{\partial \varepsilon}{\partial z})^2/(\beta_p-\beta_q)^2$. Namely,

$$|\frac{A(\beta_q,z_1)}{A(\beta_p,z_0)}|^2 \propto \int_{z_0}^{z_1}\frac{1}{(\beta_p-\beta_q)^2}\Big(\iint_S(\frac{1}{\varepsilon}\frac{\partial \varepsilon}{\partial z})\, dS\Big)^2 dz \tag{8}$$

Based on the estimation in Eq. (8), it is possible to design a curve that will mitigate the power transfer during the variation of curvature. In particular, with the equivalent index profile of curved waveguide $\varepsilon_{eq}(x,y,z) = \varepsilon(x,y)e^{2u\kappa(z)}$ and the width of waveguide much smaller than its curvature radius (*i.e.* $w = R_2 - R_1 \ll R_1$), we have

$$\Big|\frac{1}{\varepsilon}\frac{\partial \varepsilon}{\partial z}\Big| \approx \Big|2(R_2-x)\frac{\partial \kappa(z)}{\partial z}\Big| \tag{9}$$

Herein, it is apparent that a narrower waveguide is desirable to minimize the power transfer. Assuming the width of the waveguide to be unchanged, a tempting objective functional to be minimized is given by:

$$E\big[\kappa(s)\big] = \int_{z_0}^{z_1}(\frac{\partial \kappa(s)}{\partial s})^2 ds \tag{10}$$

where, for mathematical simplicity, we have replaced the z with the arc-length parameter s. This equation is the working equation used here to minimize the power transfer in a connection waveguide having evolving curvature along the connection path.

#171778 - $15.00 USD Received 3 Jul 2012; revised 6 Sep 2012; accepted 7 Sep 2012; published 20 Sep 2012

2.2. S-Bend Design

In this subsection, we apply our algorithm to design a low insertion loss S-bend connection waveguide [5]. S-bend connections waveguides occur in spiral waveguides wherein two interlaced Archimedean spirals (one clockwise and one counter clockwise) must be joined near the center of either spiral. An application of recent interest has been the creation of ultra-low optical loss waveguides for true time delay applications [23–27]. Significant efforts have been put into realization of these structures [2–4]. Recently, we have demonstrated a silica-on-silicon waveguide having optical attenuation of 0.08 dB/m over path lengths as long as 27 meters [5]. These delay-line designs feature two embedded Archimedean-shaped spirals, coupled using an S-bend waveguide [5]. In previous research [3, 4], the S-bend waveguide paths are normally constructed from sinusoidal curves, ellipses or other families of curves that are not necessarily the optimal choice. In contrast, using the above described algorithm, we can design an optimal S-bend so as to minimize excitation of higher-order modes.

We note that the functional E is the L^2 norm of the variation of curvature along the arc. This problem is therefore similar to the "minimization of variation of curvature (MVC)" problem in computer graphics and free-way design [15]. The variation of E leads to the following corresponding Euler-Lagrange equation,

$$\kappa''(s) = 0 \tag{11}$$

The solution family is $\kappa = k_0 + k_1 s$, which are similarity transformations of the basic Euler spiral (*i.e.* clothoid) $\kappa = s$ [14], where the curvature varies linearly along the length of the curve. Indeed, the Euler spiral has been employed as the transition curve in connecting straight and bent waveguides [13]. This solution is, however, unsatisfying for a variety of reasons. First, the variational equation is expressed in terms of κ rather than curve (x,y); also, the boundary conditions are expressed in terms of curvature rather than z. Similarly, positional endpoint constraints are missing. The most general endpoint constraints are the specification of curve length, end point positions, and end point tangents. Of these, the end point position constraints require Lagrange multipliers. The end point constraints (x_0,y_0) and (x_1,y_1) for connection to waveguides A and B are expressed as the integral of the unit tangent vector of direction $\theta(s)$:

$$\begin{cases} x_0 + \int_0^S \cos(\theta(s))ds = x_1 \\ x_0 + \int_0^S \sin(\theta(s))ds = y_1 \end{cases} \tag{12}$$

Therefore, by adding the Lagrange multipliers (λ_1 and λ_2) and eliminating κ in favor of θ, the following the functional must be minimized over the length l [28]

$$E' = \int_0^l \Big[(\theta'')^2 + \lambda_1 \sin\theta + \lambda_2 \cos\theta\Big] ds \tag{13}$$

The corresponding Euler-Poisson equation is then given by:

$$2\theta'''' + \lambda_1 \cos\theta - \lambda_2 \sin\theta = 0\,. \tag{14}$$

Without loss of generality we may assume $\lambda_1 = 0$ and observe that $\frac{dy}{ds} = \sin\theta$.

$$\theta'''' - \lambda_2 y' = 0\,. \tag{15}$$

Upon integration, the resulting equation is

$$\kappa'' = \lambda_2 y \tag{16}$$

#171778 - $15.00 USD Received 3 Jul 2012; revised 6 Sep 2012; accepted 7 Sep 2012; published 20 Sep 2012

where $\kappa(s) = \theta'(s)$ and the constant of integration has been set at zero by a translation of the curve. As an aside, it is interesting to note that for $\lambda_2 = 0$, this equation is equivalent to that of the Euler spiral. To approximately solve this ODE (Eq. (16)), we may consider a family of curves with curvature given in terms of a cubic polynomial of arc length "s" [28, 29].

$$\kappa(s) = a_0 + a_1 s + a_2 s^2 + a_3 s^3 . \tag{17}$$

This curve family provides a very good approximation to the original variational problem and provides an analytical expression of the connection path [28]. To see this, assuming small turning angles, y is almost proportional to s plus a constant offset, so substituting into Eq. (16), $\kappa'' \approx c_1 s + c_2$, and then integrating twice yields Eq. (17).

The coefficients of the polynomial (a_i) are determined by matching the endpoint positions,

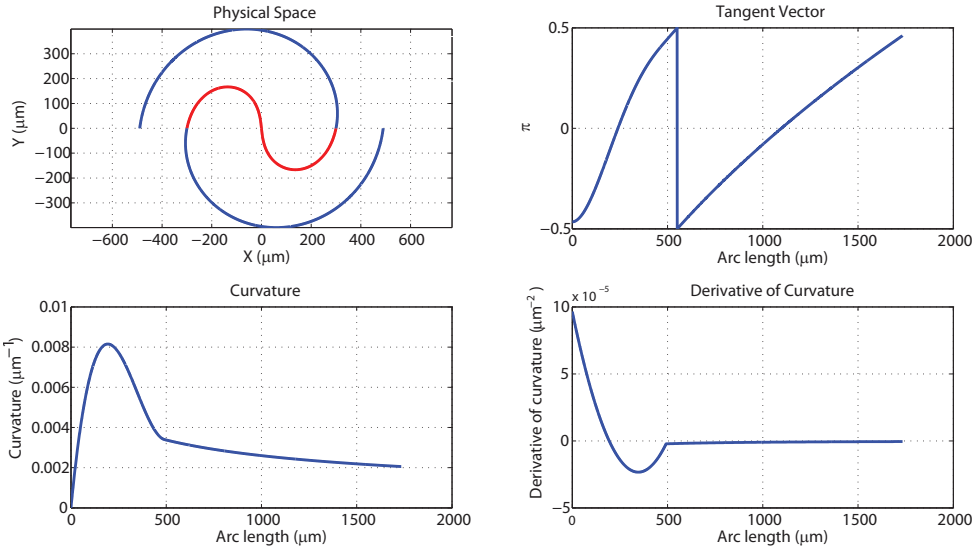

Fig. 3: The optimal S-bend design that minimizes mode coupling between clockwise and counter-clockwise Archimedean spiral waveguides. A jump from 0.5π to -0.5π of the tangent vector in the upper right panel is due to the convention that the tangent vector is defined as $[-0.5\pi, 0.5\pi]$ (for example, a tangent vector of 0.6π is considered as $0.6\pi - \pi = -0.4\pi$). The geometry property is still continuous.

endpoint tangents and the curvature between the S-bend and Archimedean spiral. By symmetry, we only need to design the incoming arc of the S-bend. This curve starts at the origin $(x = 0, y = 0)$ and has curvature $\kappa = 0$ at $x = 0, y = 0$, which leads to the following formulation

$$\begin{cases} \theta_1 = \theta_0 + \int_0^{s_1} \kappa(s) ds = \theta_0 + \int_0^{s_1} a_1 s + a_2 s^2 + a_3 s^3 \, ds \\ \kappa_1 = a_1 s + a_2 s^2 + a_3 s^3 |_{s=s_1} \\ \kappa_1' = \frac{d\kappa(s)}{ds}\Big|_{s=s_1} = \frac{d}{ds}\left(a_0 + a_1 s + a_2 s^2 + a_3 s^3\right)\Big|_{s=s_1} \\ (x_1, iy_1) = \int_0^{s_1} \exp(i\theta(s)) ds \end{cases} \tag{18}$$

The additional constraint of curvature at the starting point has been enforced and gives $a_0 = 0$. By solving a set of unknowns $(a_1, a_2, a_3, \theta_0, s_1)$ to match the input parameters

#171778 - $15.00 USD Received 3 Jul 2012; revised 6 Sep 2012; accepted 7 Sep 2012; published 20 Sep 2012

$(\theta_1, \kappa_1, \kappa_1', (x_1, iy_1))$ from the end point of the Archimedean spiral, a curve for the adiabatic coupler is successfully defined as shown is Fig. 3.

3. Experimental Verification

Measurement of connector loss in waveguides is complicated by the insertion loss associated with coupling light into the waveguide. To avoid this problem entirely we use optical backscatter reflectometry [30]. The spiral waveguides and S connector waveguide are fabricated via procedures outlined in Ref. [5]. This process begins with lithography and etching with buffered hydrofluoric acid of silica on silicon. The oxide layer then functions as an etch mask for an isotropic dry etch of the silicon using XeF_2. Further details on the processing are given in Ref. [5]. Figure. 4(a) shows a 7 m (physical length) spiral waveguide that is approximately 4.5 cm in diameter. The angle-cleaved input facet (7 degree cleave angle) is at the upper left corner of the chip. Optical fiber and index-matching oil are used for end-fire coupling. The waveguides have a width of 170 microns. A magnification of the S-shaped connection is shown in Fig. 4(b). The connection width was tapered to 10 microns at its narrowest point to relax the condition in Eq. (9). The spiral waveguides were characterized using a Luna OBR 4400 backscatter reflectometer [30]. A measured backscatter trace is given in Fig. 4(c). As can be seen in the trace, the adiabatic connector creates a singularity in the backscattering signal. Higher-resolution measurement of this singularity reveals that this region rises and plateaus over a length of several mm at the center of the S-bend connection (see inset to Fig. 4(c)). The apparent lack of any decrease in backscatter signal within this region required that another method be applied to analyze the coupler loss.

As an alternate measurement, we plotted the ratio of out-going to in-going backscatter strength at equidistant points from the spiral center. By symmetry, these pairs of points will have the same curvature. The ratio of backscatter strength can be written as

$$\log\left(\frac{P_{backscatter}(\frac{z}{2})}{P_{backscatter}(-\frac{z}{2})}\right) = -\alpha_1 \cdot z - \alpha_0 \tag{19}$$

where the center of the spiral is the origin, $P_{backscatter}(\frac{z}{2})$ and $P_{backscatter}(-\frac{z}{2})$ are out-going and in-coming waveguide backscattering strength at the equidistant points from the spiral center; the waveguide length between these two points is z; α_1 is the waveguide loss per unit length and α_0 is the insertion loss of the S-bend connection. Such a plot is shown in Fig. 4(d). The slope of the linear fit gives approximately 0.35 dB/m loss for the waveguide, while the intercept gives an estimated insertion loss for the adiabatic coupler of 0.05 dB. This insertion loss and the indicated confidence interval result from linear regression on all of the points. Data points within 0.25 meters of the S-bend have been omitted in this estimate as there is a large increase in the variance on account of the steep slope associated with the backscatter singularity (see Fig. 4(c)). As an aside, the spiral device of this measurement was fabricated using a contact aligner and therefore features a higher waveguide loss as compared to that reported in Ref. [5], wherein devices were fabricated using a Canon stepper lithography tool.

To evaluate the spectral performance of the connection, backscattering measurements were performed over $1536 - 1598$ nm with an instrument measurement window set to 10 nm. Figure. 5 shows the spectral dependence of the intercept (see Fig. 4(d)) measured in a 1 meter spiral. There is, overall, a weak variation across the spectrum, however, the variation is larger than that inferred from the confidence interval in Fig. 4(d). We attribute this to the reduced length of this spiral and hence the smaller number of points used in the regression. Reducing the measurement window to 10 nm to study the spectral variation is also believed to have contributed to a larger variation.

#171778 - $15.00 USD Received 3 Jul 2012; revised 6 Sep 2012; accepted 7 Sep 2012; published 20 Sep 2012

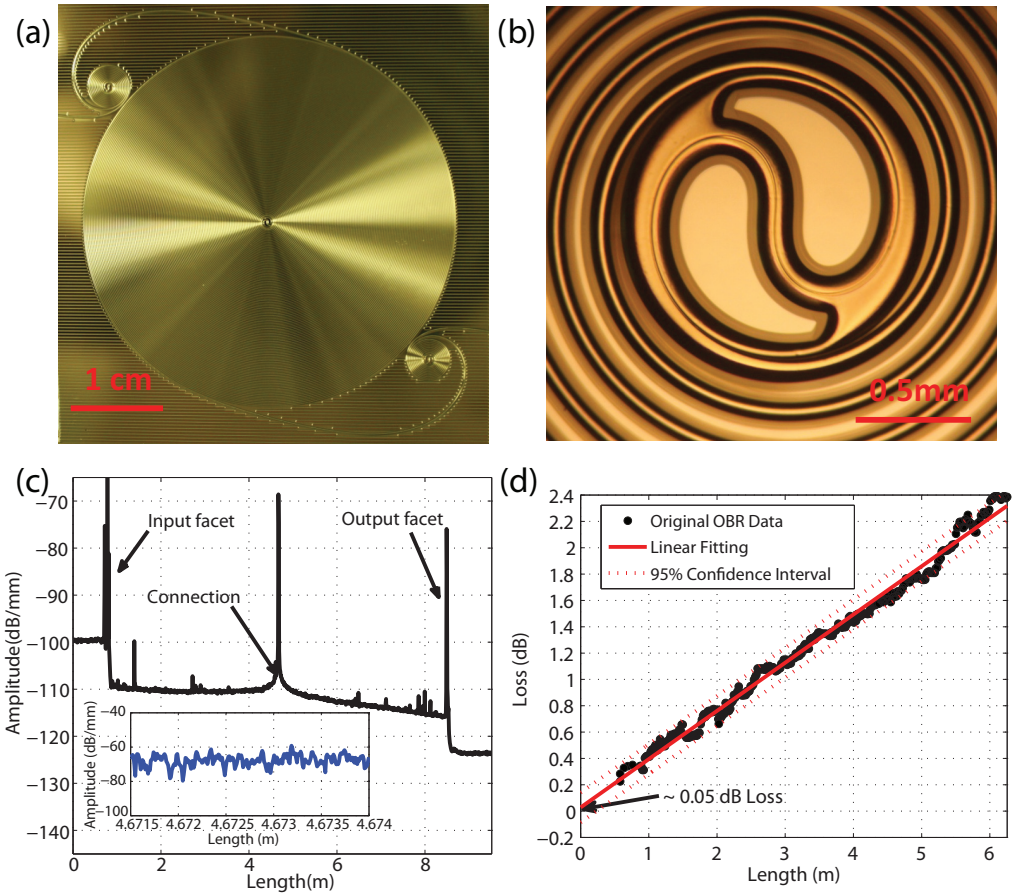

Fig. 4: **(a)** Optical micrograph of a spiral waveguide having a physical path length of 7 meters. The input port is in the upper left of the image, and there are two small spirals at the input and output ports (not resolved in the backscatter trace of panel (c)). The entire chip is 4.5 cm $\times$ 4.5 cm. **(b)** A magnified view of the adiabatic coupling section (approximately 1 mm in diameter). Light brown regions are silicon (under oxide or exposed) while darker brown regions along the border of the light brown are silica that has been undercut by dry etching. Very-dark-brown border regions are also silica but having a wedge profile. For further details see Ref. [5]. **(c)** Optical backscatter reflectometer measurement of the spiral waveguide. Besides occasional random noise spikes that we believe are associated with small dust particles on the surface of the waveguide, the major singularities in the backscatter signal correspond to the input facet, the optical wave transiting the inner adiabatic coupling region of the spiral and the output facet. The inset shows a close-in view of the adiabatic coupler region (*i.e.*, peak of the singularity). There is no apparent drop in signal within this region. **(d)** Analysis of the adiabatic coupler insertion loss using backscatter data. Data points are generated by taking the ratio of backscatter signals at symmetrically offset distances away from the adiabatic coupler in (a). The intercept reveals the insertion loss of the S connection as given by a range of possible values falling within a confidence interval determined by linear regression.

#171778 - $15.00 USD Received 3 Jul 2012; revised 6 Sep 2012; accepted 7 Sep 2012; published 20 Sep 2012

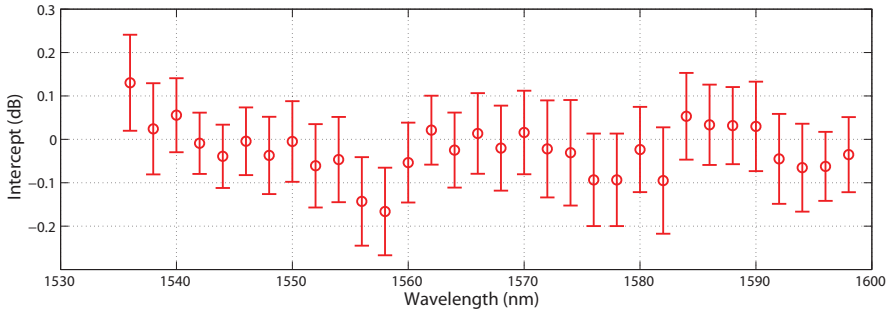

Fig. 5: The S connection intercept (see Fig. 4(d)) measured with backscattering reflectometry over a wavelength range from 1536 to 1598 nm in a 1 meter long spiral waveguide. A measurement window of 10 nm is applied. The error bars are obtained from three independent measurements.

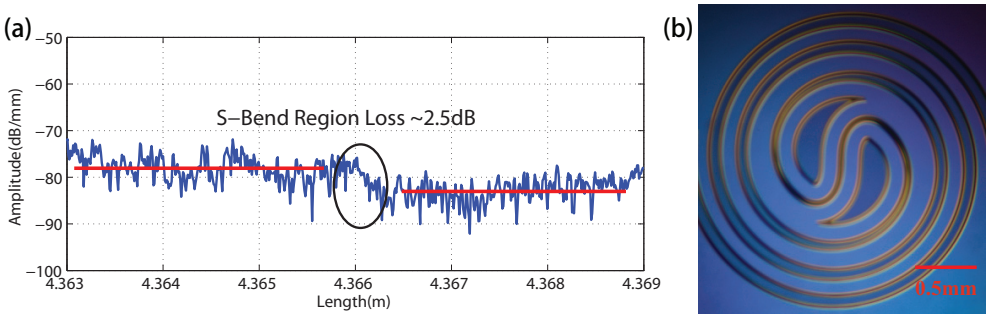

Fig. 6: **(a)** A high-spatial-resolution, backscatter trace of an unsuccessful S-bend design based on a conventional clothoid curve design. About 2.5 dB insertion loss was measured using the OBR measurement technique. **(b)** Micrograph of the clothoid curve S connection.

In our S-connector design, the waveguide length of connection is approximately 1 cm (with waveguide width $10\,\mu m$). We compared measured insertion loss to attenuation calculations based upon atomic force microscope (AFM) roughness data [5,31]. It shows that surface roughness scattering is the principle source of attenuation in the S connection [31], and the surface scattering loss is estimated to be 1.8 dB/m based on a model outlined in Ref. [5]. The increase in waveguide loss within the S-connection as compared to the Archimedean section of the spiral waveguide is a result of the reduced width of the S connection waveguide. This width, as noted earlier, was reduced so as to relax the adiabaticity condition.

Finally, we also characterized a S-connection design using a traditional clothoid curve. As shown in Fig. 6(a), a 2.5 dB insertion loss was inferred from high spatial resolution OBR measurements. This should be compared to the similar measurement (see inset in Fig. 4(c)) performed on the structure in Fig. 4(a). In that measurement no drop in backscatter level was observable. A micrograph of the clothoid connection is provided in Fig. 6(b). The clothoid curve starts at the origin (defined here as the center of the spiral) with zero curvature and its

#171778 - $15.00 USD Received 3 Jul 2012; revised 6 Sep 2012; accepted 7 Sep 2012; published 20 Sep 2012

curvature varies linearly with its arc-length. The other end of the clothoid needs to connect smoothly to the outside Archimedean spiral smoothly, which is not a trivial task and can introduce extra loss. The clothoid curve data were obtained using a tapered fiber coupler [32, 33] to couple to the interior arc (as opposed to end-fire coupling). This approach enables rapid testing of the structures.

4. Conclusion

We have presented a variational approach to design of adiabatic optical waveguide connections. This algorithm is based on a coupled mode theory and minimizes the inter-mode power coupling by appropriate design of curvature along a variational path. This optimization process can be implemented automatically and incorporated into mask-generating software. At the same time, it is general enough to cover most situations in optical circuit designs that connect two arbitrary waveguides. Because the approach is based on continuous adjustments to curvature it is less sensitive to dimension control in etching/fabrication of the waveguide in comparison with the offset approach. Meanwhile, the loss of the designed connector is insensitive to wavelength and provides good performance over a broad-band spectrum.

As a demonstration, a S-bend connector for spiral waveguides was designed and fabricated. Backscattering measurements confirmed the excellent performance over 65 nm in the telecommunication band. The measured loss originated mainly from surface scattering.

Acknowledgments
We gratefully acknowledge the Defense Advanced Research Projects Agency under the iPhoD program, the Institute for Quantum Information and Matter, an NSF Physics Frontiers Center with support of the Gordon and Betty Moore Foundation, and also the Kavli Nanoscience Institute at Caltech. H. L. thanks the Center for the Physics of Information.

#171778 - $15.00 USD Received 3 Jul 2012; revised 6 Sep 2012; accepted 7 Sep 2012; published 20 Sep 2012